

ChemComm

Accepted Manuscript



This is an *Accepted Manuscript*, which has been through the Royal Society of Chemistry peer review process and has been accepted for publication.

Accepted Manuscripts are published online shortly after acceptance, before technical editing, formatting and proof reading. Using this free service, authors can make their results available to the community, in citable form, before we publish the edited article. We will replace this *Accepted Manuscript* with the edited and formatted *Advance Article* as soon as it is available.

You can find more information about *Accepted Manuscripts* in the [Information for Authors](#).

Please note that technical editing may introduce minor changes to the text and/or graphics, which may alter content. The journal's standard [Terms & Conditions](#) and the [Ethical guidelines](#) still apply. In no event shall the Royal Society of Chemistry be held responsible for any errors or omissions in this *Accepted Manuscript* or any consequences arising from the use of any information it contains.

Light-responsive peptide [2]rotaxanes as gatekeepers of mechanised nanocontainers

Received 00th January 20xx,
Accepted 00th January 20xx

A. Martinez-Cuezva, S. Valero-Moya, M. Alajarin and J. Berna*

DOI: 10.1039/x0xx00000x

www.rsc.org/

Novel mechanized silica nanoparticles incorporating a peptide-based molecular shuttle as a photo-responsive interlocked gatekeeper of nanocontainers are described including the uptake and delivery studies of a model cargo.

Since the beginning of this century the use of mesoporous materials for the smart delivery of cargoes has been an appealing research topic.^{1,2} In these studies systems devoted to the controlled release of drugs have a singular significance due to their promising therapeutic use.³ In this arena, mesoporous silica nanoparticles (MSNs) have become an outstanding material for controlled delivery applications due to their exceptional features as high loading capacity, wide diversity regarding size, shape and pore diameter, easy functionalization, mechanical and chemical resistance and biocompatibility.^{4,5} Numerous stimuli-responsive methods⁶ have been established to govern the trapping and liberation of small molecules from the pores of these nanocontainers incorporating different organic or inorganic motifs behaving as blockers or gatekeepers. One promising group of these tailor-made doors is based on threaded/interlocked structures⁷ giving rise to the materials known as mechanized silica nanoparticles⁸ which have been seen as intelligent materials with an excellent potential for the advance of novel nanodosifiers.⁹ Typically, the benefits of the MSNs and the well-known templating method to assemble MCM-41 make this silica support the preferred choice for probing the ability of [2]pseudorotaxanes or bistable [2]rotaxanes to act as controllable gates of their pores. In this regard, a variety of mechanized silica has been investigated having different macrocyclic component, including cyclophanes,¹⁰ crown ethers,¹¹ cucurbiturils¹² and cyclodextrins,¹³ as gatekeepers of these nanocontainers. To the best of our knowledge, the positional switching of benzylic amide rings have never been tested as an open/close mechanism for controlling the release and capture of cargoes from MSNs.

Among the [2]rotaxanes containing a benzylic amide macrocycle pioneered by Leigh,^{7b-e} the subset of the peptide-based structures¹⁷ are considered excellent scaffolds for the building of a broad range of molecular shuttles,¹⁴ logic gates,¹⁵ information storage devices¹⁶ and enzymatic delivery systems of bioactive compounds.¹⁷

Herein, we describe the preparation of novel mechanized silica nanoparticles having a peptide-based molecular shuttle as a photocontrollable gatekeeper and MCM-41 as mesoporous support aimed to the construction of light-operated nanocontainers. The

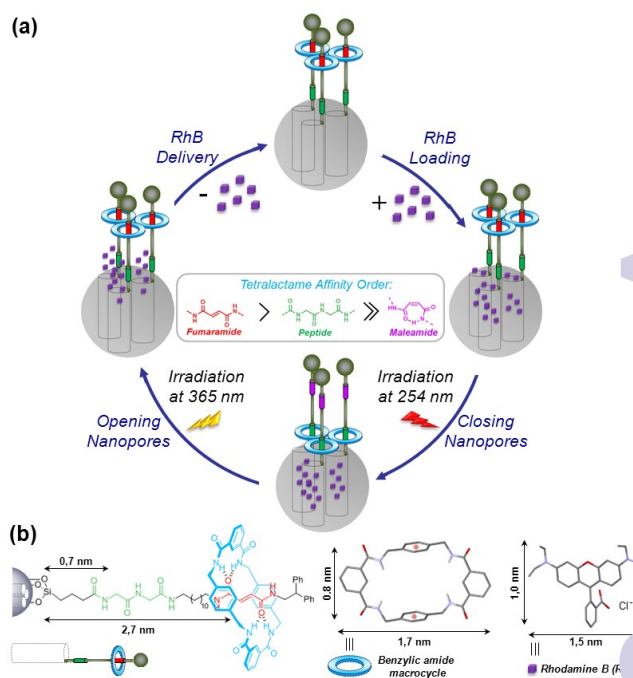


Fig. 1 (a) Uptake and release of dye cargo molecules (RhB) from the pores of a MCM-41 silica functionalized with a light-responsive peptide [2]rotaxane. The movable lid is tetralactame which locates on the preferred station (fumaramide, red cylinder, peptide, green cylinder) depending on its affinity order. (b) Relative distance of the silicon atom to the first HB acceptor of the stations which are connected by the thread, illustrating the feasibility of the RhB loading. Cross dimensions (in nm) of the sealing tetralactame (blue ring) and the RhB cargo molecule (purple block) showing up the size matching with the average diameter (ca 2 nm) of nanopores of the silica support. Molecular modeling structures of macrocycle and RhB cation are shown. Distances values were obtained from CCDC database (see reference 20).

Departamento de Química Orgánica, Facultad de Química, Regional Campus of International Excellence "Campus Mare Nostrum", Universidad de Murcia, E-30100, Murcia, Spain. E-mail: ppberna@um.es

† Electronic Supplementary Information (ESI) available: Synthetic procedures, experimental details and characterization. See DOI: 10.1039/x0xx00000x

loading and delivery of rhodamine B (RhB) as model cargo through the mechanism depicted in Fig. 1 is also reported.

Our system is based on the light-induced *E/Z* isomerization of a fumaramide-based binding site for shuttling the macrocycle along the thread of a bistable [2]rotaxane¹⁸ thus closing and opening a molecular gate in the surface of a mesoporous silica support. We placed a peptide station (green cylinder, Fig. 1a) nearby to the silica surface and connected to a fumaramide station (red cylinder) by an alkyl chain. In the open-pore state, the tetralactame ring is located on the fumaramide station allowing the free diffusion of the cargo RhB molecules (purple blocks) toward the void of the pores. The photoisomerization of the olefin affording the maleamide derivative (pink cylinder) alters the binding affinity of the unsaturated station by several kilocalories per mole¹⁹ and promotes the ring translocation towards the peptide-based binding site for entrapping the cargo (Fig. 1a). A *cis-to-trans* olefin isomerization shuttles back the ring to the fumaramide station thus opening the pores for enabling the release of the RhB molecules and allowing the reusability of these nanocontainers.

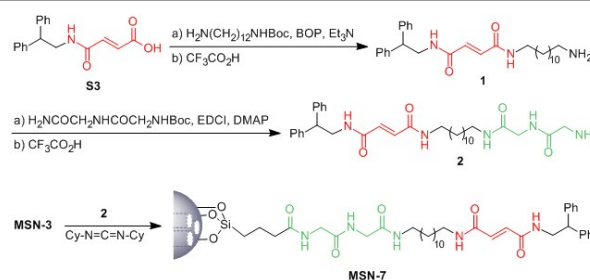
The matching of the porous mesostructure of the silica nanoparticles (*ca* 100-200 nm diameter) containing hexagonally arranged pores (*ca* 2 nm diameter) and the relative sizes²⁰ of the model cargo (RhB: 1.0 x 1.5 nm) and the ring (benzylc tetralactame: 0.8 x 1.7 nm) supports the ability of the latter for keeping the cargo molecules inside the pores (Fig. 1b). In addition, the relative distance of each station of the [2]rotaxane respect to porous surface regulates the position of moveable lid and, consequently, it determines the limiting cross dimensions of the loading cargo molecules to be larger than 0.7 nm but shorter than 2.7 nm.

Tetraethylortosilicate as silicon source and cetyltrimethylammonium bromide (CTAB) as template were used in a base-catalyzed sol-gel protocol²¹ for affording the mesostructured silica of the MCM-41 type (**MSN-1**). The size and the mesoporous structure of the nanoparticles were studied by scanning electron and transmission electron microscopies, respectively (see Fig. S1a,b).

The final **MSN-E-6** system was assembled in a stepwise synthesis from the thermoactivated²² silica nanoparticles (Scheme 1). First, the spherical surface of **MSN-1** was functionalized with nitrile functions affording **MSN-2** by heating with 2-cyanoethyltriethoxysilane in toluene. Further refluxing with 50% sulfuric acid

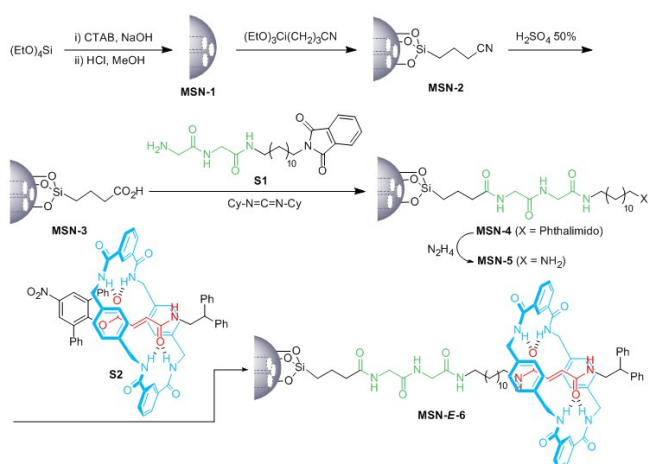
provided the surface-bound carboxylic acid **MSN-3**. Next, amide bond formation between the carboxy groups of **MSN-3** with the glycolglycine building block **S1** (see ESI) in the presence of *N,N*-dicyclohexylcarbodiimide afforded the corresponding phthalimide functionalized particles **MSN-4**. Subsequent hydrazinolysis²³ of the preceding silica provided the amino-functionalized **MSN-5** which was completely separated from the phthalhydrazide byproduct by continuous extraction in a Soxhlet apparatus with hot ethanol. Finally, the nucleophilic substitution of the bulky 2,6-diphenyl-4-nitrophenoxy stopper^{17a} of the fumaramide rotaxane **S2** (see ESI) by the amino groups of the latter silica particles yielded the target **MSN-E-6** with a surface gated with a two-station peptide [2]rotaxane (Scheme 1).

Non-mechanized nanoparticles **MSN-7** bearing an identical linear fragment to that of **MSN-E-6** were also prepared according to the synthetic route outlined in Scheme 2. In this regard, the amine was prepared through a two consecutive amide coupling and deprotection protocol for incorporating the fumaramide and peptide binding sites tethered by a dodecyl alkyl chain. Next, carbodiimide-mediated amide formation between the acid-terminated surface of **MSN-3** and the amine **2** led to silica nanoparticles **MSN-7** which were used as a non-threaded model material, lacking of the benzylc amide macrocycle.



Scheme 2 Synthesis of the mesoporous silica nanoparticles **MSN-7** functionalized with the two-binding site thread precursor **2**.

The structure determination and characterization of the compounds and materials shown in the Schemes 1 and 2 were accomplished by means of their analytical and spectral data (see ESI). Although intense bands of the Si-O-Si stretching and bending vibrations at 1080 and 800 cm^{-1} are present in the FTIR spectra of all the silica materials shown in these schemes (see Figs. S3, S4) the functional groups incorporated in each stage are also evidenced in these spectra. Thus, the spectrum of **MSN-3** shows a weak band at 2953 cm^{-1} owned to the C-H stretch and a strong one at 1726 cm^{-1} corresponding to the C=O stretching vibration of the carboxy group. At the end of the transformations outlined in Scheme 1, the FTIR spectrum of the interlocked **MSN-E-6** shows two intense C=O bands at 1646 and 1540 cm^{-1} corresponding to the C=O stretching vibrations of the different amido groups of the gatekeeper, also displaying intense bands in the range of 2983 and 2894 cm^{-1} due to the methylene groups present in this motif. ²⁹Si and ¹³C cross polarization magic-angle spinning solid-state (SS) NMR spectroscopies were also used to examine the grafting and attaching of the different organic fragments into MCM-41. The ²⁹Si SSNMR spectrum (see Fig. S5) of the silica **MSN-2** shows two T signals at -54.8 and -61.9 ppm corresponding to the silicon atoms directly connected to the organic fragments and a Q signal at -



Scheme 1 Synthesis of the mesoporous silica nanoparticles **MSN-E-6** functionalized with a photocontrollable peptide [2]rotaxane.

109.5 ppm ascribed to the rest of silicon atoms $[\text{Si}(\text{OSi})_n(\text{OH})_{4-n}]$; $n = 2-4$). The measurement of the ^{13}C SSNMR spectrum of each of new synthesized material confirmed the successive chemical transformations toward the final mechanized silica (see ESI). The spectrum of the targeted **MSN-E-6** shows several sets of signals at different chemical shift ranges: at 174.1-163.3 ppm appear those corresponding to the carbon atoms of the carbonyl groups of the amide functions, at 144.8-116.4 ppm those of the aromatic carbon atoms and at the region between 70 and 10 ppm come out those of the aliphatic carbon atoms (see Fig. S7). The comparison of this ^{13}C SSNMR spectra with the one of the non-interlocked **MSN-7** material displays noticeable differences evidencing the lack of the tetralactame in this latter material (see Fig. S7) further proving the functionalization of **MSN-E-6**. Finally, TGA and elemental analysis allowed to roughly estimate the maximum amount of these interlocked motifs on the surface of **MSN-E-6** as being approximately 0.30 mmol per gram of silica.

Next the light-responsive gating behavior of **MSN-E-6** was investigated. The diffusion of the RhB cargo into the pores of this light-responsive silica was carried out by soaking the mechanized nanoparticles in a stirred aqueous solution of the guest compound for 24 h. The surface-adsorbed excess of the cargo was thoroughly washed and the resulting material was carefully dried. Then the pores of the material were sealed by means of a *trans*-to-*cis* photoisomerization of the olefin station^{14c,18,24} by irradiation at 254 nm promoting the shifting of the tetralactame ring toward the peptide station close to the surface of the nanoparticulated silica. This operation kinetically entraps the guest molecules into the **MSN-Z-6** container and, then, the RhB loaded silica is thoroughly washed and dried. Although the accessibility of the cargo to the pores of the **MSN-1** decreased after its functionalization with the rotaxane, as it was confirmed by TEM observation (see Fig. S14), the openings of the gated material still permitted the entrance of enough RhB for carrying the study of its controlled release.

The delivery of RhB from the nanopores of **MSN-Z-6** was investigated in two different solvents, dichloromethane and water. For closely related interlocked systems¹⁸ it is known that the polarity of the solvent affects to the position of the ring over the peptide binding site. Thus, whereas in non-disrupting hydrogen bond solvents as such dichloromethane the ring is mainly located on the peptide station, in polar solvents the alkyl chain would act as a second solvophobic station.¹⁸ For this purpose, a stirred suspension of the RhB-loaded **MSN-Z-6** was irradiated at 365 nm for promoting the *cis*-to-*trans* isomerization which triggers the ring translocation to the most energetically favorable binding site that, in this case, is the resulting fumaramide station far away from the surface of the nanoparticulated silica. Consequently, this latter irradiation promotes the opening of the pores and the release of RhB, which was monitored by measuring the absorbance spectrum at different times (Fig. 2, inset). The obtained profile for the light-driven opening of the gatekeepers of this silica in dichloromethane shows a progressive delivery of the cargo reaching a 50% of the maximum delivery in 50 min and needing 30 min more to reach a liberation of 80% of the cargo (Fig 2a). Using Beer-Lambert's law, the RhB loading was calculated revealing that, for 3 mg of RhB-loaded **MSN-Z-6**, 0.175 μmol (2.8 wt %) of cargo was released (see ESI).

When the release experiment was carried out in water, the discharge of half the load lasted 200 min and the release profile for the rest is extended for more than 5 h (Fig 2b). Consequently the remarkable positional integrity of the ring after photoisomerization of the maleamide binding site to its *trans* isomer promotes the expected release of the cargo in dichloromethane, and less quickly in water due to the decrease of the ring discrimination. At this point it is convenient to remark that slow dynamics release profiles as that shown in Fig 2b are desirable in therapeutic treatments as it allows a moderated liberation of potent (and/or short half-life) drugs.^{2,3}

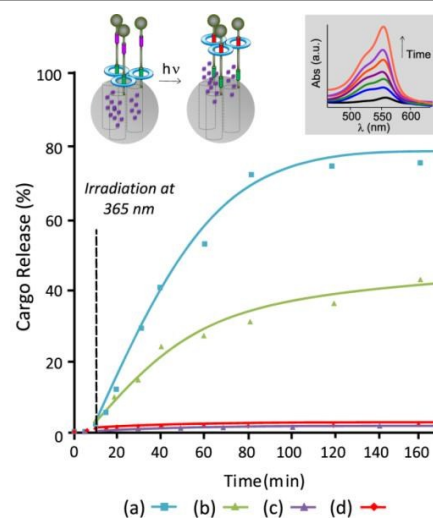


Fig. 2 Comparison of the release profiles of RhB from **MSN-Z-6** in dichloromethane solution (a, c) and aqueous solution (b, d). These experiments were carried out at 25 °C under light irradiation at 365 nm (a,b) and without photoactivation (c,d). The inset displays the absorbance spectral change at 553 nm after the irradiation with 365 nm light of a suspension of RhB-loaded **MSN-Z-6**.

It also should be noted that the interlocked nanogates of this container prevent significant premature releases of the cargo dye molecules as revealed by the flat region (0-10 min) of the profiles in both solvents (Fig. 2a,b). We also carried out control experiments by monitoring the absorbance of RhB-loaded **MSN-Z-6** in absence of light in both studied solvents (Fig 2c,d), showing the absence of leaking processes under such conditions. Incidentally, these latter results also give an idea of the positional integrity of the ring over the peptide-based binding site in **MSN-Z-6** (see ESI). Release control experiments with the non-mechanized material RhB-loaded **MSN-1** disclosed a quick leaking of the guest molecules into solution confirming the key role of the benzylic amide macrocycle as the interlocked gatekeeper of **MSN-6** (see ESI).

In summary, we have demonstrated the feasibility of building mechanized silica nanoparticles using a peptide-based molecular shuttle and MCM-41 as mesoporous support. We have shown the efficiency of this particular functionalization in actuating a gatekeepers upon exposure to a visible light irradiation displaying different dosages depending on the working conditions. The unprecedented integration of a benzylic tetralactame as a movable lid allows a proficient uptake and release of RhB employed as model cargo. This mechanized material must be included to the yet scarce number of described light-operated molecular nanovalves and opens stimulating opportunities for the development of a novel

generation of smart nanocontainers by anchoring amide-based interlocked compounds which could be used as controlled delivery systems.

This work was supported by the MINECO (CTQ2009-12216/BQU and CTQ2014-56887-P) and Fundacion Seneca-CARM (Project 19240/PI/14). A.M.-C. thanks the Marie Curie COFUND / U-IMPACT programs and the MINECO for his postdoctoral contracts. We also thank Prof. José M. González and Dr. Almudena Torres of the National Center for Electron Microscopy (UCM, Madrid) for their helpful assistance with the TEM observations.

Notes and references

- 1 T. Torres and G. Bottari, Eds., in *Organic Nanomaterials*, Wiley, Hoboken (US) 2013.
- 2 (a) A. P. Wight and M. E. Davis, *Chem. Rev.*, 2002, **102**, 3589–3613; (b) L. Nicole, C. Laberty-Robert, L. Rozes and C. Sanchez, *Nanoscale*, 2014, **6**, 6267–6292; (c) N. Linares, A. M. Silvestre-Albero, E. Serrano, J. Silvestre-Albero and J. Garcia-Martinez, *Chem. Soc. Rev.*, 2014, **43**, 7681–7717; (d) S. Alberti, G. J. A. A. Soler-Illia and O. Azzaroni, *Chem. Commun.*, 2015, **51**, 6050–6075.
- 3 (a) M. Vallet-Regi, F. Balas and D. Arcos, *Angew. Chem., Int. Ed.*, 2007, **46**, 7548–7558; (b) M. Vallet-Regi, M. Colilla and B. Gonzalez, *Chem. Soc. Rev.*, 2011, **40**, 596–607; (c) M. Colilla and M. Vallet-Regi, *Smart Mater. Drug Deliv.*, 2013, **2**, 63–89.
- 4 (a) C. Argyo, V. Weiss, C. Bräuchle and T. Bein, *Chem. Mater.*, 2014, **26**, 435–451; (b) A. Baeza, M. Colilla and M. Vallet-Regi, *Expert Opin. Drug Deliv.*, 2015, **12**, 319–337.
- 5 For some recent studies of biocompatible MSNs with exceptional cargo delivery properties see: (a) S. R. Gayam and S.-P. Wu, *J. Mater. Chem. B*, 2014, **2**, 7009–7016; (b) P. Pakawanit, S. Ananta, T. K. Yun, J. Y. Bae, W. Jang, H. Byun and J.-H. Kim, *RSC Adv.*, 2014, **4**, 39287–39296; (c) Y.-J. Cheng, G.-F. Luo, J.-Y. Zhu, X.-D. Xu, X. Zeng, D.-B. Cheng, Y.-M. Li, Y. Wu, X.-Z. Zhang, R.-X. Zhuo and F. He, *ACS Appl. Mater. Interfaces*, 2015, **7**, 9078–9087.
- 6 (a) B. G. Trewyn, I. I. Slowing, S. Giri, H.-T. Chen and V. S.-Y. Lin, *Acc. Chem. Res.*, 2007, **40**, 846–853; (b) E. Aznar, R. Martinez-Mañez and F. Sancenon, *Expert Opin. Drug Deliv.*, 2009, **6**, 643–655; (c) C. Coll, A. Bernardos, R. Martinez-Mañez and F. Sancenon, *Acc. Chem. Res.*, 2013, **46**, 339–349.
- 7 (a) D. B. Amabilino and J. F. Stoddart, *Chem. Rev.*, 1995, **95**, 2725–2829; (b) E. R. Kay, D. A. Leigh and F. Zerbetto, *Angew. Chem., Int. Ed.*, 2007, **46**, 72–191; (c) W. Yang, Y. Li, H. Liu, L. Chi and Y. Li, *Small*, 2012, **8**, 504–516; (d) M. Xue, Y. Yang, X. Chi, X. Yan and F. Huang, *Chem. Rev.*, 2015, DOI: 10.1021/cr5005869; (e) D.-H. Qu, Q.-C. Wang, Q.-W. Zhang, X. Ma and H. Tian, *Chem. Rev.*, 2015, DOI: 10.1021/cr5006342.
- 8 (a) K. K. Coti, M. E. Belowich, M. Liang, M. W. Ambrogio, Y. A. Lau, H. A. Khatib, J. I. Zink, N. M. Khashab and J. F. Stoddart, *Nanoscale*, 2009, **1**, 16–39; (b) M. W. Ambrogio, C. R. Thomas, Y.-L. Zhao, J. I. Zink and J. F. Stoddart, *Acc. Chem. Res.*, 2011, **44**, 903–913; (c) Y. W. Yang, Y. L. Sun and N. Song, *Acc. Chem. Res.*, 2014, **47**, 1950–1960.
- 9 (a) C. Y. Ang, S. Y. Tan and Y. Zhao, *Org. Biomol. Chem.*, 2014, **12**, 4776–4806; (b) X. Ma and Y. Zhao, *Chem. Rev.*, 2015, DOI: 10.1021/cr500392w
- 10 (a) R. Hernandez, H. R. Tseng, J. W. Wong, J. F. Stoddart and J. I. Zink, *J. Am. Chem. Soc.*, 2004, **126**, 3370–3371; (b) T. D. Nguyen, H.-R. Tseng, P. C. Celestre, A. H. Flood, Y. Liu, J. F. Stoddart and J. I. Zink, *Proc. Natl. Acad. Sci. U. S. A.*, 2005, **102**, 10029–10034.
- 11 (a) T. D. Nguyen, K. C.-F. Leung, M. Liang, C. D. Pentecost, J. F. Stoddart and J. I. Zink, *Org. Lett.*, 2006, **8**, 3363–3366; (b) T. D. Nguyen, Y. Liu, S. Saha, K. C.-F. Leung, J. F. Stoddart and J. I. Zink, *J. Am. Chem. Soc.*, 2007, **129**, 626–634.
- 12 For examples containing CB[6] rings see: (a) C. R. Thomas, P. Ferris, J.-H. Lee, E. Choi, M. H. Cho, E. S. Kim, J. F. Stoddart, J.-S. Shin, J. Cheon and J. I. Zink, *J. Am. Chem. Soc.*, 2010, **132**, 10623–10625; (b) M. Wang, T. Chen, C. Ding and J. Fu, *Chem. Commun.*, 2014, **50**, 5068–5071. For recent examples containing CB[7] rings see: (c) Y. L. Sun, B. J. Yang, S. X. Zhang and Y. W. Yang, *Chem. - Eur. J.*, 2012, **18**, 9212–9216; (d) J. Fu, T. Chen, M. Wang, N. Yang, S. Li, Y. Wang and X. Li, *ACS Nano*, 2013, **7**, 11397–11408. For a recent example containing CB[8] rings see: (e) C. Hu, Y. Lan, F. Tian, K. R. West and O. A. Scherman, *Langmuir*, 2014, **30**, 10926–10932.
- 13 For recent examples containing α -CD rings see: (a) Z. Luo, X. Ding, Y. Hu, S. Wu, Y. Xiang, Y. Zeng, B. Zhang, H. Yan, H. Zhang, L. Zhu, J. Liu, J. Li, K. Cai and Y. Zhao, *ACS Nano*, 2017, **7**, 10271–10284; (b) D. Tarn, D. P. Ferris, J. C. Barnes, M. W. Ambrogio, J. F. Stoddart and J. I. Zink, *Nanoscale*, 2014, **6**, 3335–3343. For some examples containing β -CD rings see: (c) Y.-L. Zhao, Z. Li, S. Kabehie, Y. Y. Botros, J. F. Stoddart and J. I. Zink, *J. Am. Chem. Soc.*, 2010, **132**, 13016–13025; (d) Wang, Z. Li, D. Cao, Y.-L. Zhao, J. W. Gaines, O. A. Bozdemir, M. W. Ambrogio, M. Frascioni, Y. Y. Botros, J. I. Zink and J. F. Stoddart, *Angew. Chem., Int. Ed.*, 2012, **51**, 5460–5465; (e) M. D. Yilmaz, M. Xue, M. W. Ambrogio, O. Buyukcikir, Y. Wu, M. Frascioni, X. Chen, M. S. Nassar, J. F. Stoddart and J. I. Zink, *Nanoscale*, 2015, **7**, 1067–1072.
- 14 (a) A. S. Lane, D. A. Leigh and A. Murphy, *J. Am. Chem. Soc.*, 1997, **119**, 11092–11093; (b) G. W. H. Wurpel, A. M. Brouwer, I. H. M. van Stokkum, A. Farran and D. A. Leigh, *J. Am. Chem. Soc.*, 2001, **123**, 11327–11328; (c) G. Bottari, D. A. Leigh and E. M. Perez, *J. Am. Chem. Soc.*, 2003, **125**, 13360–13361.
- 15 D. A. Leigh, M. A. F. Morales, E. M. Perez, J. K. Y. Wong, C. Saiz, A. M. Z. Slawin, A. J. Carmichael, D. M. Haddleton, A. M. Brouwer, W. J. Buma, G. W. H. Wurpel, S. Leon and F. Zerbetto, *Angew. Chem., Int. Ed.*, 2005, **44**, 3062–3067.
- 16 M. Cavallini, F. Biscarini, S. Leon, F. Zerbetto, G. Bottari and D. A. Leigh, *Science*, 2003, **299**, 531.
- 17 (a) A. Fernandes, A. Viterisi, F. Coutrot, S. Potok, D. A. Leigh, V. Aucagne and S. Papot, *Angew. Chem., Int. Ed.*, 2009, **48**, 6443–6447; (b) A. Fernandes, A. Viterisi, V. Aucagne, D. A. Leigh and S. Papot, *Chem. Commun.*, 2012, **48**, 2083–2085; (c) R. Barat, T. Legigan, I. Tranoy-Opalinski, B. Renoux, E. Péraudeau, J. Clarhaut, P. Poinot, A. E. Fernandes, V. Aucagne, D. A. Leigh and S. Papot, *Chem. Sci.*, 2015, **6**, 260.
- 18 E. M. Perez, D. T. F. Dryden, D. A. Leigh, G. Teobaldi and F. Zerbetto, *J. Am. Chem. Soc.*, 2004, **126**, 12210–12211.
- 19 (a) A. Altieri, G. Bottari, F. Dehez, D. A. Leigh, J. K. Y. Wong and F. Zerbetto, *Angew. Chem., Int. Ed.*, 2003, **42**, 2296–2300; (b) G. Bottari, F. Dehez, D. A. Leigh, P. J. Nash, E. M. Perez, J. K. Y. Wong, and F. Zerbetto, *Angew. Chem., Int. Ed.*, 2003, **42**, 5886–5889.
- 20 These cross dimensions are average values resulting from the crystallographic distances of related structures included in the CCDC database, CSD 5.36 update Feb 2015.
- 21 S. Huh, J. W. Wiench, J.-C. Yoo, M. Pruski, and V. S.-Y. Lin, *Chem. Mater.*, 2003, **15**, 4247–4256.
- 22 A. J. Butterworth, J. H. Clark, P. H. Walton and S. J. Barlow, *Chem. Commun.*, 1996, 1859–1860.
- 23 Preliminary studies revealed that the hydrazinolysis, in a number of reaction conditions (N_2H_4 or $MeNHNH_2$), on a closely related material to **MSN-4** but containing a Glycyl ester function as that incorporated in the reported molecular shuttle in ref. 18 resulted in a decomposition of the starting material instead of the exclusive expected amine formation.
- 24 P. Altoe, N. Haraszkiwicz, F. G. Gatti, P. G. Wiering, C. Frochot, A. M. Brouwer, G. Balkowski, D. Shaw, S. Woutersen, W. J. Buma, F. Zerbetto, G. Orlandi, D. A. Leigh, and M. Garavelli, *J. Am. Chem. Soc.*, 2009, **131**, 104–117.